Precision-cut tissue slices: a novel ex vivo model for fibrosis research

Pham, Bao Tung

Chapter 6

Precision-cut kidney slices (PCKS) to study development of renal fibrosis and efficacy of drug targeting *ex vivo*

F. Poosti, B. T. Pham, D. Oosterhuis, K. Poelstra,
H. van Goor, P. Olinga, J.L. Hillebrands

Disease Models and Mechanisms 2015, 8(10), 1227-1236.

ABSTRACT

Background: Renal fibrosis is a serious clinical problem forming the utmost cause of need for renal replacement therapy. No adequate preventive or curative therapy is available that can be clinically used to specifically target renal fibrosis. The search for new efficacious treatment strategies is therefore warranted. Although *in vitro* models using homogeneous cell populations have contributed to the understanding of the pathogenetic mechanisms involved in renal fibrosis, these models poorly mimic the complex *in vivo* milieu. Therefore, here we evaluated a precision-cut kidney slice (PCKS) model as a new, multicellular *ex vivo* model to study development of fibrosis and the prevention thereof using antifibrotic compounds.

Methods: Precision-cut slices (200-300 μm thickness) were prepared from healthy C57BL/6 mouse kidneys using a Krumdieck tissue slicer. To induce changes mimicking the fibrotic process, slices were incubated with TGFβ1 (5 ng/ml) for 48 h in the presence or absence of the antifibrotic cytokine IFNγ (1 μg/ml) or an IFNγ conjugate which is targeted to the PDGFRβ (PPB-PEG-IFNγ). Following culture, tissue viability (ATP-content) and expression of α-SMA, fibronectin, collagen I, and collagen III were determined using real-time PCR and immunohistochemistry.

Results: Slices remained viable up to 72 h of incubation and no significant effects of TGFβ1 and IFNγ on viability were observed. TGFβ1 markedly increased α-SMA, fibronectin, and collagen I mRNA and protein expression levels. IFNγ and PPB-PEG-IFNγ significantly reduced TGFβ1-induced fibronectin, collagen I and collagen III mRNA expression which was confirmed by immunohistochemistry.

Conclusions: The PKCS model is a novel tool to test the pathophysiology of fibrosis and to screen the efficacy of antifibrotic drugs *ex vivo* in a multicellular and pro-fibrotic milieu. Major advantage of the slice model is that it can be used not only for animal but also for (fibrotic) human kidney tissue.

INTRODUCTION

Renal fibrosis is a major contributor to the development of chronic kidney disease (CKD) and is characterized by accumulation of myofibroblasts and excessive extracellular matrix deposition (Eddy, 2011; Friedman et al., 2003). CKD culminates in End-Stage Renal Disease (ESRD) eventually, resulting in significant morbidity and mortality for which the only available therapy is dialysis or renal transplantation (Levey et al., 2007). The pathophysiology of renal fibrosis is not fully understood and hitherto no adequate preventive or curative therapy is clinically available (Boor et al., 2010). Research focusing on unraveling the pathophysiology of renal fibrosis is therefore warranted. Traditionally, renal research is performed in *in vitro* cell culture systems or small rodent models as well as on human renal biopsies or explants (Westra et al., 2013). Despite the fact that *in vitro* experiments using homogeneous single cell preparations allow functional analyses of a specific cell type, the major disadvantage obviously is lack of cell heterogeneity and cellular microarchitecture; phenomena that are undoubtedly involved in determining and driving the fibrotic process (Vickers et al., 2005; Westra et al., 2013). Because of ethical constraints, the use of animal models is increasingly discouraged. Furthermore, use of human tissue biopsies is by definition descriptive in nature and prohibits functional studies.

The availability of an *ex vivo* model system that does allow functional analyses on the development of renal fibrosis is therefore highly desired. Recently, precision cut tissue slices (PCTS) have been increasingly used to study the development of liver fibrosis (Hadi et al., 2013; Westra et al., 2014a; Westra et al., 2014b). In this model cell-cell and cell-extracellular matrix interactions are preserved. As yet, it is unknown whether precision-cut kidney slices (PCKS) can be used to study the development of renal fibrosis and to screen the efficacy of antifibrotic compounds, e.g. IFNγ. IFNγ is a pleiotropic cytokine produced by various activated immune cells including NK cells and T cells (Farrar and Schreiber, 1993). In addition to its pro-inflammatory effects, IFNγ has prominent antifibrotic effects. IFNγ is able to inhibit fibroblast activation and proliferation, and also reduces extracellular matrix synthesis (Lee et al., 2013; Oldroyd et al., 1999; Strutz et al., 2000; Weng et al., 2005; Yao et al., 2011). These properties make IFNγ a potential molecule for therapeutic use to target fibrosis. However, the short half-life and undesirable systemic side effects clearly limit clinical utility of IFNγ as an antifibrotic drug (Cleland et al., 1996; Gu

et al., 2005; King et al., 2009). To overcome these problems, we employed a drug-targeting strategy in which IFNγ was targeted specifically to activated myofibroblasts in animal models of liver and kidney fibrosis using the PDGFRβ as docking receptor for the PPB-PEG-IFNγ conjugate (PPB: PDGFRβ-recognizing receptor) (Bansal et al., 2011a; Bansal et al., 2011b; Bansal et al., 2011c; Bansal et al., 2012; Poosti et al., 2014).

The aim of the present study was to validate the precision-cut kidney slice (PCKS) model for the development of TGFβ1-induced renal fibrosis and to evaluate the potential antifibrotic effects of IFNγ and PPB-PEG-IFNγ in this *ex vivo* model.

RESULTS

Viability of mouse kidney slices (mPCKS) during incubation

In order to determine viability of mPCKS, ATP levels per mg of protein were assessed directly after preparation of slices, and after 1, 6, 12, 24, 48, and 72 h of incubation (Figure 1A). Kidney slices remained viable up to 72 h of incubation; however, a minor, non-significant decrease in ATP levels was observed after 24 h of incubation. Up to 72 h slices retained constant ATP levels. Since the morphology of kidney slices started to deteriorate after 72 h of incubation (based on PAS staining, data not shown), the experiments with TGFβ1 and antifibrotic compounds were conducted with a maximal culture time of 48 h. In a separate experiment, we first examined the viability of slices after 48 h of incubation with or without TGFβ1 in the presence of free IFNγ, PPB-PEG-IFNγ or PPB-HSA. As shown in Figure 1B, TGFβ1 did not significantly alter ATP content. Furthermore, free IFNγ, PPB-PEG-IFNγ, or PPB-HSA did not affect ATP levels independent of presence or absence of TGFβ1.

Uptake of FITC-lysozyme by mPCKS

We next analyzed whether exogenously added proteins can reach the center of mPCKS during incubation. As model protein we used FITC-conjugated lysozyme. As shown in Figure 1C, after 1 h of incubation, FITC-conjugated lysozyme was only present at the outer surface area of mPCKS. However, after 3 h of incubation fluorescence was detected throughout the thickness of the slices with high staining intensity (depicted in green) also observed within the center of the slice.

Biological activity of IFNγ and PPB-PEG-IFNγ ex vivo

To determine the biological activity of free IFNγ and PPB-PEG-IFNγ, we assessed major histocompatibility class II (*MHC II*) expression which is known to be upregulated by IFNγ (Bansal et al., 2011a). Expression of *MHC II* in response to IFNγ was analyzed in TGFβ- and non-TGFβ-incubated slices. qRT-PCR results showed that incubation of kidney slices in the presence of both free IFNγ and PPB-PEG-IFNγ caused a significant upregulation of MHC II expression compared with

medium, effects that were not influenced by TGFβ1 (Figure 2A). However, PPB-HSA (the PDGFRβ-specific drug delivery carrier without IFNγ) did not induce *MHC II* expression. These data indicate that IFNγ and PPB-PEG-IFNγ retained their biological activity in kidney slices.

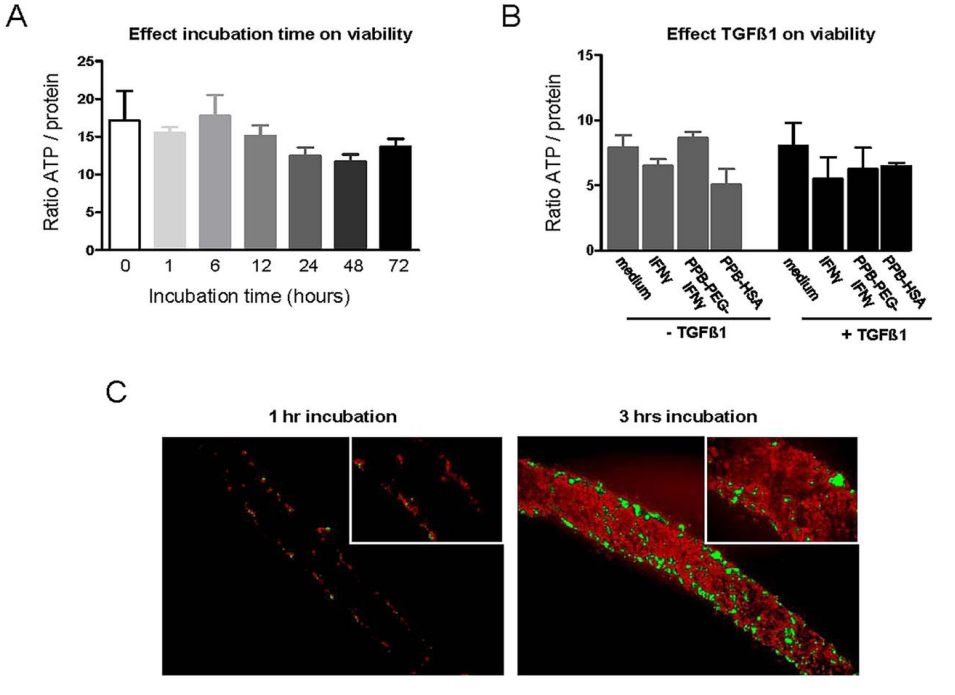

Figure 1. Effect of incubation time and conditions on mPCKS viability, and uptake of FITC-lysozyme by mPCKS. (A) Non-cultured normal kidney slices (n = 3) directly after the slicing procedure (0) and after different incubation intervals. (B) Effect of 48 h of incubation with TGFβ1 on ATP content of mPCKS in the presence of IFNγ, PPB-PEG-IFNγ and PPB-HSA with or without TGFβ1. (C) mPCKS were incubated with FITC-lysozyme (model protein) for 1 h (left panel) and 3 h (right panel) to determine penetration of exogenously added protein in mPCKS (magnification: 100×, inset: 400×).

PDGFRβ expression in mPCKS

We recently showed increased interstitial *PDGFRβ* expression in both human and mouse fibrotic renal tissue which co-localized with α-SMA positive interstitial myofibroblasts (Poosti et al., 2015). High expression of *PDGFRβ* on interstitial myofibroblasts indicates that this receptor is an appropriate target for fibroblast-specific delivery. Therefore, we next analyzed whether cultured mPCKS

in the presence of TGFβ1 are also characterized by *PDGFRβ* expression. As shown in Figure 2B, mPCKS cultured with medium but without TGFβ1 clearly expressed *PDGFRβ* which was not increased by TGFβ1. A clear, but non-significant reduction in *PDGFRβ* expression was observed after incubation in the presence of free IFNγ and PPB-PEG-IFNγ (Figure 2B).

Induction of α-SMA and ECM expression in mPCKS by TGFβ1

To study development of (pre)fibrosis in mPCKS in the presence of TGFβ1, mRNA expression of fibrosis markers was determined after 48 h of incubation with TGFβ1 (5 ng/ml). As shown in Figure 3, we observed significant upregulation of *α-SMA* (A), *fibronectin* (B), and *collagen I* (C) mRNA expression upon incubation with TGFβ1 compared to non-TGFβ1 incubated control (medium) slices. TGFβ1 also increased expression of *collagen III*, however without reaching the level of statistical significance ($p = 0.08$). We next tested by immunohistochemistry whether increased mRNA expression of fibrosis markers also translated into altered protein expression levels. As shown in Figure 4A (two upper rows), incubation with TGFβ1 indeed markedly increased α-SMA, fibronectin and collagen III expression.

Effect of free IFNγ and PPB-PEG-IFNγ on the expression of fibrosis markers

To investigate whether free IFNγ and PPB-PEG-IFNγ treatment ameliorates fibrosis, qRT-PCR analysis was performed on fibrotic and healthy control slices. As already shown in Figure 3, TGFβ1 induced *α-SMA*, *fibronectin*, *collagen I*, *and collagen III* mRNA expression. Figure 5A depicts a schematic representation of the targeting strategy in which IFNγ is targeted towards PDGFRβ-expressing myofibroblasts using the PPB-PEG-IFN**γ** conjugate. In cultured slices incubated with TGFβ plus either IFN**γ** or PPB-PEG-IFN**γ**, mRNA expression levels for *fibronectin*, *collagen I*, and *collagen III* were significantly reduced compared to slices incubated with TGFβ alone (Figure 5C-E). IFNγ and PPB-PEG-IFNγ also showed somewhat reduced *α-SMA* expression (Figure 5B), however without reaching the level of statistical significance. To determine whether IFNγ, PPB-PEG-IFNγ, and PPB-HSA have protective effects in spontaneous induction of fibrosis, kidney slices were also incubated with the aforementioned compounds in the absence of TGFβ1. In this condition, we did not observe significant reduction of fibrosis maker expression in

the presence of free IFNγ or PPB-PEG-IFNγ, although clear trends were observed for *collagen I* (Figure 5D) and *collagen III* (Figure 5E).

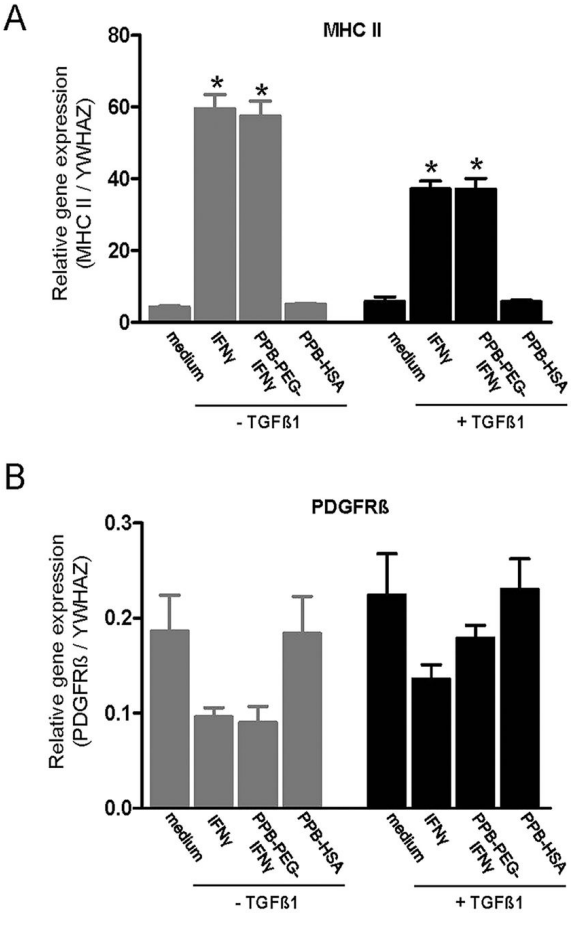

Figure 2. *MHC II* and *PDGFRβ* expression in mPCKS. (A) mRNA expression of *MHC II* in pre-fibrotic (+TGFβ1) and non-fibrotic (−TGFβ1) kidney slices treated with IFNγ, PPB-PEG-IFNγ or PPB-HSA. (B) mRNA expression of *PDGFRβ* in pre-fibrotic (+TGFβ1) and non-fibrotic (−TGFβ1) kidney slices treated with IFNγ, PPB-PEG-IFNγ or PPB-HSA. *$p < 0.05$ versus medium.

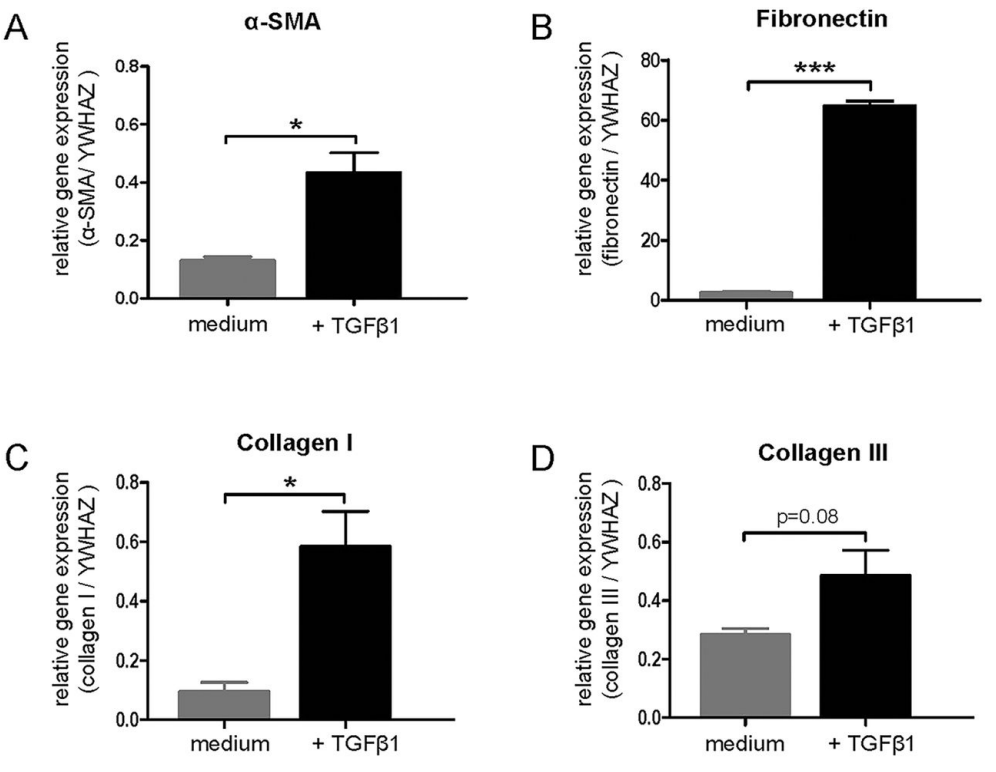

Figure 3. TGFβ1 (5 ng/ml) induces expression of fibrotic markers in mPCKS. mRNA expression of (A) α-SMA, (B) *fibronectin*, (C) *collagen I* and (D) *collagen III* in mouse kidney slices after 48 h of incubation. *$p < 0.05$, ***$p < 0.001$ versus medium.

To determine whether mRNA expression profiles also translated into differential protein expression levels, immunohistochemistry for α-SMA, fibronectin and collagen III was performed. Staining for collagen I was technically not feasible. Representative photomicrographs of α-SMA, fibronectin and collagen III staining are shown in Figure 4A. Microscopic analysis revealed no clear differences in α-SMA expression (similar to mRNA expression, Figure 3B). Quantitative analysis for fibronectin (Figure 4B) showed significantly ($p < 0.01$) increased expression levels in slices cultured in the presence of TGFβ1 (compared with medium) which was reduced by IFNγ ($p < 0.05$) and PPB-PEG-IFNγ ($p = 0.05$). Similar results were observed for the expression of collagen III (Figure 4C). PPB-HSA did not show any significant inhibitory effect on neither mRNA nor protein levels.

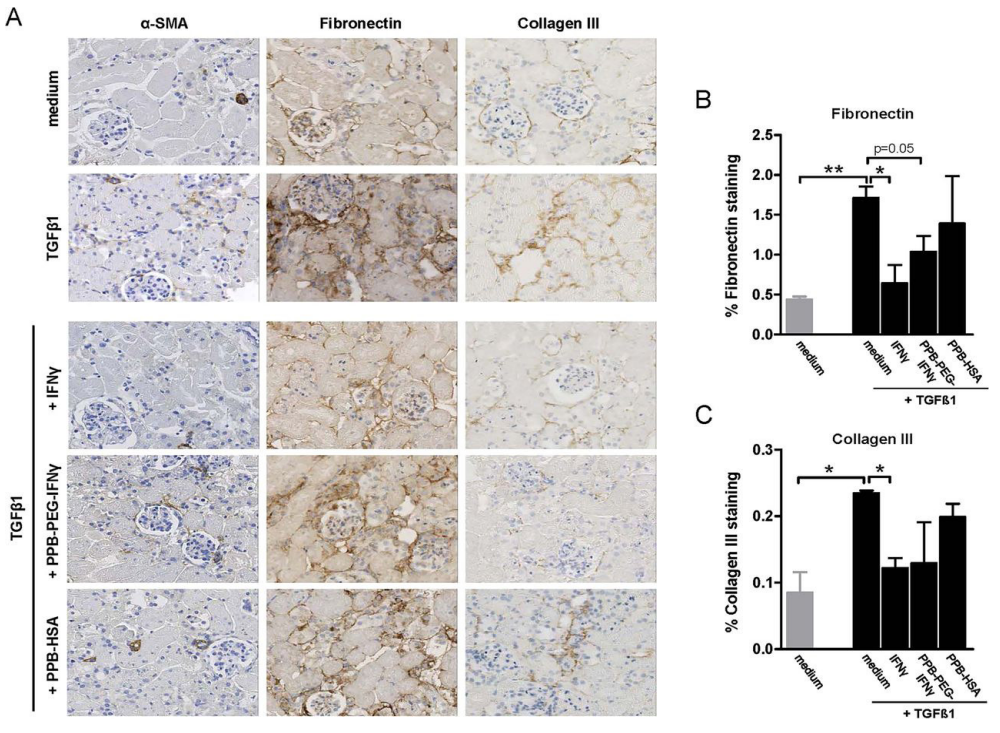

Figure 4. Protein expression of α-SMA, fibronectin and collagen III in mPCKS cultured without TGFβ (medium), or with TGFβ in the presence of free IFNγ, PPB-PEG-IFNγ or PPB-HSA. (A) Photomicrographs of immunohistochemistry for α-SMA, fibronectin and collagen III on mPCKS after 48 h of culture (magnification: 200×). Quantitative analysis of fibronectin (B) and collagen III (C) expression in mPCKS cultured under various conditions. *$p < 0.05$, **$p < 0.01$; Student's t-test.

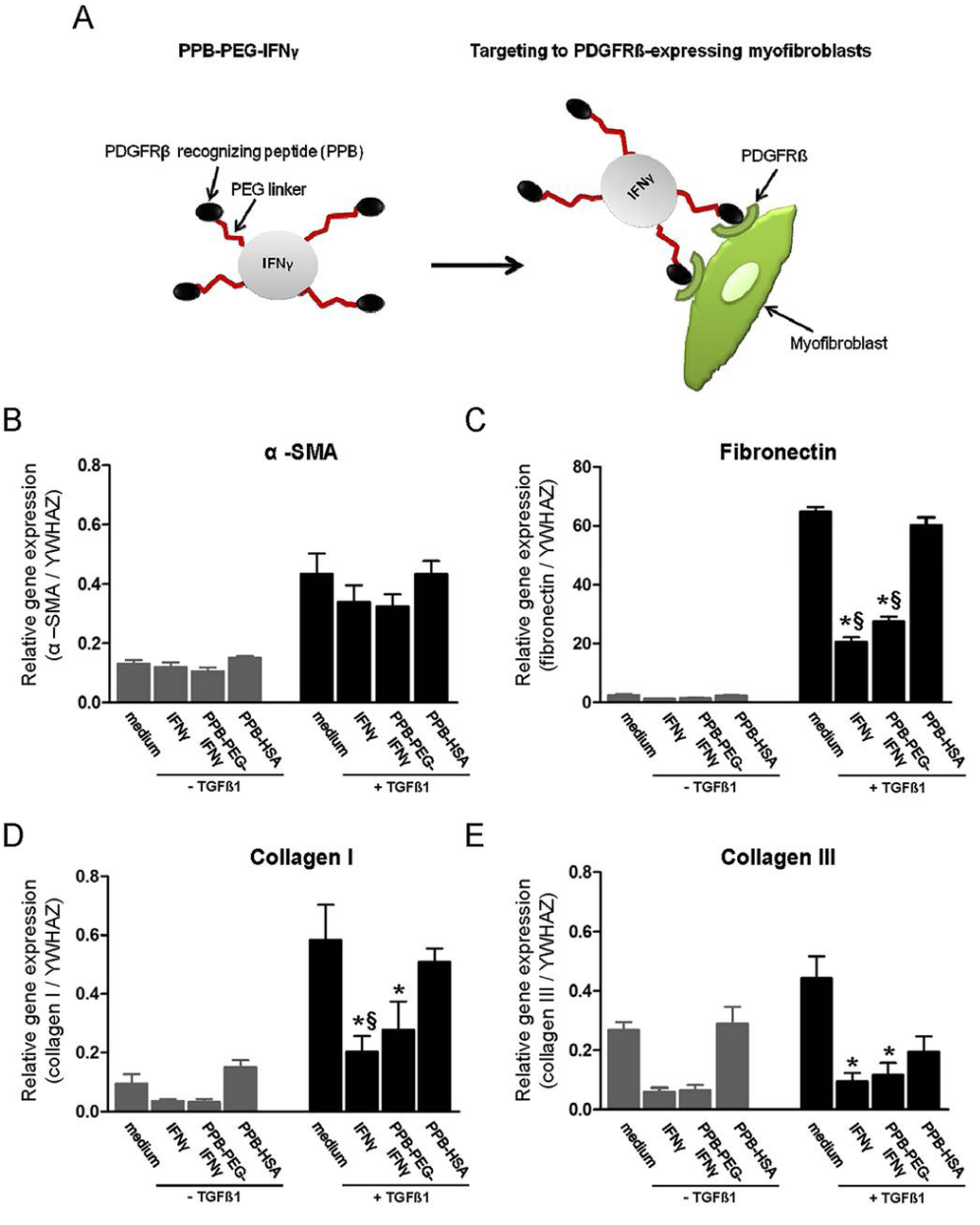

Figure 5. Effect of IFNγ and PPB-PEG-IFNγ on the expression of fibrotic markers in mPCKS. (A) Schematic of targeted delivery of IFNγ to PDGFRβ-expressing myofibroblasts in mPCKS. Relative gene expression of (B) α-SMA, (C) *collagen I*, (D) *fibronectin* and (E) *collagen III*. *$p < 0.05$ versus medium; §$p < 0.05$ versus PPB-HSA.

DISCUSSION

The present study reveals the applicability of precision-cut kidney slices (PCKS) as: 1) an *ex viv*o model to study renal fibrogenesis, and 2) to test antifibrotic effects of IFNγ and targeted IFNγ aiming at reducing renal fibrosis. Specifically, the results demonstrate that incubation of mPCKS with TGFβ1 resulted in upregulation of *fibronectin*, *collagen I* and *α-SMA* expression which indicates that mPCKS represent an ideal model to study the onset of early fibrosis. Preserved expression of α-SMA suggests that fibroblasts remained active during culture, still intervention with free IFNγ and PPB-PEG-IFNγ clearly dampened TGFβ1-induced expression of *fibronectin*, *collagen I* and *collagen III*, thereby demonstrating the antifibrotic potential of both free and targeted IFNγ.

Renal fibrosis results from excessive extracellular matrix accumulation and fibroblast proliferation (Duffield, 2014; LeBleu et al., 2013; Strutz and Zeisberg, 2006). In order to develop an efficacious antifibrotic therapy, detailed knowledge of the underlying pathophysiology is necessary. It is already recognized for long time that *in vitro* studies can provide useful information on the mechanisms of disease (Westra et al., 2013; Westra et al., 2014a). PCTS, a three-dimensional multicellular environment, is a powerful model in order to provide insight into mechanisms of organ injury (Basile et al., 2012; Flamant et al., 2006; Nagae et al., 2008; Tharaux et al., 2000; van Swelm et al., 2014). Tissue slices have the biologically relevant structural features of *in vivo* tissues (de Kanter et al., 2002). PCTS have been widely used as *ex vivo* model to study development of liver and intestinal fibrosis (de Kanter et al., 2005). *Ex vivo* liver and intestinal slices maintain cell heterogeneity and tissue architecture, providing an appropriate tool to study multicellular processes such as fibrosis (de Kanter et al., 2005; van de Kerkhof et al., 2005; Westra et al., 2014b; de Graaf et al., 2010).

In this study mouse kidney slices remained viable during the incubation period of 72 h, as determined by ATP content, a parameter generally used as indicator of viability. In addition, the increased expression of fibrosis markers in response to TGFβ1 also indicated that the relevant cells involved in fibrogenesis *(i.e.*, fibroblasts) remained viable. It is generally accepted that stimulation with TGFβ1 induces differentiation of local fibroblasts into myofibroblasts which start to produce and secrete extracellular matrix. In line with this, we recently demonstrated

that the same concentration of TGFβ1 (5 ng/ml) as used in current study induces collagen and α-SMA expression in NIH3T3 fibroblasts indicating TGFβ1-induced fibroblast to myofibroblast differentiation (Poosti et al., 2015). Although other renal cell types (including tubular epithelial cells, endothelial cells, podocytes, mesangial cells and pericytes) may also respond to TGFβ1 (Meng et al., 2015), our immunohistochemistry data support tubulointerstitial (myo)fibroblasts as main responders to TGFβ1 in mPCKS. Activation and/or proliferation of fibrogenic cells, which was accompanied by increased production of extracellular matrix, indicates that kidney slices could be a useful tool to study the effects of antifibrotic compounds in a multicellular environment.

IFNγ could be a useful therapeutic target to attenuate the development of renal fibrosis. Despite its potential effectiveness, application of IFNγ in clinical trials resulted in negative data (Cleland et al., 1996; Gu et al., 2005; King et al., 2009). The main reasons for the lack of clinical effects is the poor pharmacokinetic profile of IFNγ and the severe side effects due to ubiquitous expression of IFNγ receptors. Therefore, targeted delivery of IFNγ to key cells is thought to be a prerequisite to enhance its therapeutic efficacy and at the same time reduce systemic side effects. Recently, we studied antifibrotic effects of IFNγ and PEGylated IFNγ (PPB-PEG-IFNγ) targeted to PDGFRβ-expressing myofibroblasts in an animal model of renal fibrosis (Poosti et al., 2014). Our strategy was to conjugate the cyclic PDGFRβ-binding peptide (PPB) to mouse IFNγ via a PEG linker (PPB-PEG-IFNγ) to achieve specific delivery of IFNγ to PDGFRβ-expressing cells, due to upregulation of this receptor in fibrotic diseases. In order to check the applicability of the PCKS model for testing antifibrotic compounds, we examined IFNγ and targeted IFNγ (PPB-PEG-IFNγ) on TGFβ-activated pre-fibrotic slices and on non-activated slices. Contrary to our expectation, PDGFRβ expression was not affected by TGFβ1. This might be explained by the fact that fibrosis is a multifactorial process, and therefore induction of PDGFRβ expression *in vivo* might be dependent on presence of different pro-fibrotic cytokines rather than TGFβ1. Interestingly, in the group treated with IFNγ and PPB-PEG-IFNγ, we noticed a trend towards reduction of PDGFRβ expression which might explain their antifibrotic effects via down regulation of the PDGF/PDGFRβ signaling pathway. We observed that both IFNγ and PPB-PEG-IFNγ exert antifibrotic effects as they significantly dampened TGFβ-induced fibronectin, collagen I and collagen III expression after 48 h incubation. These observations

confirmed our recent *in vivo* data (Poosti et al., 2015). However, in contrast to these *in vivo* data, in the current study PPB-PEG-IFNγ did not show higher efficacy when compared with free IFNγ. This can be explained by the fact that TGFβ1 did not increase PDGFRβ expression on mPCKS as described above. Besides, there is usually no added benefit of targeted compounds *in vitro*, since compounds can easily and effectively access the target cells, which is not the case after *in vivo* administration. Similar results were also obtained after exposure of NIH3T3 fibroblasts to IFNγ and PPB-PEG-IFNγ in the presence of TGFβ1 (Poosti et al., 2015). In fact, an effect after receptor-mediated endocytosis (as for PPB-PEG-IFNγ) sometimes may even be slower than a pharmacological effect of compounds directly to its receptor. The *ex vivo* studies with PPB-PEG-IFNγ therefore demonstrate that the targeted construct is pharmacologically active and was included as proof of concept.

To determine whether the antifibrotic effects were not due to PPB-induced blockade of PDGFRβ-signaling, we coupled PPB to albumin (HSA). We did not observe remarkable antifibrotic effects of PPB-HSA *ex vivo*; only on the mRNA level a (non-significant) effect of PPB-HSA on *collagen III* expression was observed, indicating that most of the observed antifibrotic effects are IFNγ-mediated. Biological effects of IFNγ take place via the nuclear signaling sequence (NLS) which is present in the C-terminus region of IFNγ. IFNγ containing NLS is capable to bind to IFNγ receptor1 (IFNγR1) and initiate a cascade of events which is required for nuclear import of STAT1 and generation of biological activity. Activation of STAT1 by PEG-PPB-IFNγ was previously shown (Bansal et al., 2011a). We propose that PEG-PPB-IFNγ is taken up via PDGFRβ and the internalized construct next releases IFNγ or its metabolite which then binds to the intracellular part of IFNγR1 and activates the JAK/STAT pathway. However, this premise needs to be further explored.

In summary, the mPCKS model is a novel tool to study the pathophysiology of early fibrotic processes not only in animal tissue, but also in (fibrotic) human kidney tissue. Importantly, from the results of this study we conclude that the *in vivo* observed antifibrotic effect of IFNγ and PPB-PEG-IFNγ can be successfully reproduced to great extent using mPCKS. This indicates that this *ex vivo* model is a useful tool for preclinical studies to test the efficacy of potential new antifibrotic drugs on fibroblast activation in a multicellular, pro-fibrotic milieu. In addition, the use of this model can contribute substantially to the reduction, refinement, and potential replacement of animal experiments (the '3R' principles). Further studies

are ongoing to investigate the application of non-fibrotic and fibrotic human PCKS in order to validate our targeting strategy in the human setting. We believe the PCKS model is able to bridge the gap between basic research performed using *in vitro* cell culture systems and translational human *in vivo* studies as schematically represented in Figure 6. The preclinical studies using PCKS should then pave the road towards clinical studies on cell-specific targeting of renal fibrosis.

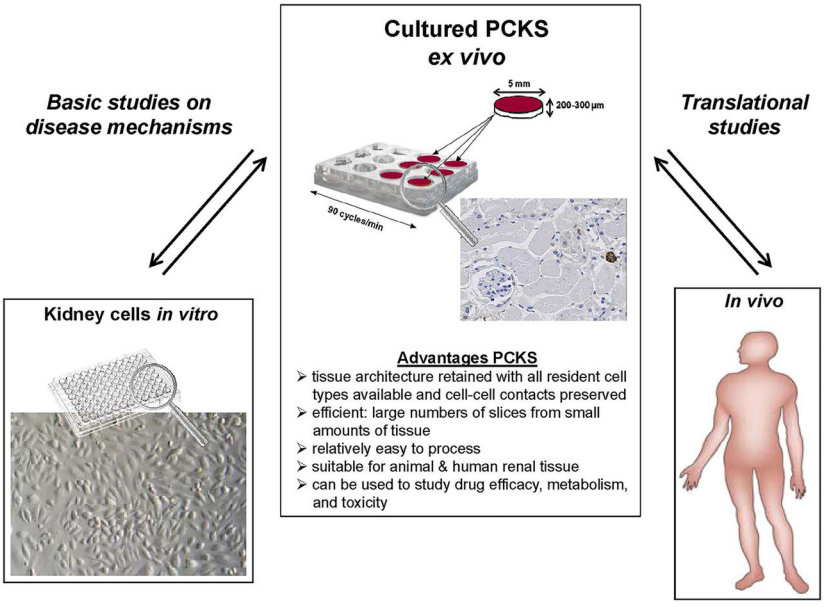

Figure 6. The *ex vivo* PCKS model bridges the gap between basic research performed in *in vitro* cell culture models and translational *in vivo* human studies on pathophysiology and therapy of renal disease. *In vitro* cultured cells displayed are primary human tubular epithelial cells (PTECs).

MATERIALS AND METHODS

Mice

Male C57BL/6 mice weighing 25-30 g were obtained from Harlan (Zeist, the Netherlands). Animals were housed in individual cages with free access to food and water. Before starting the experiment, animals were allowed to acclimatize for at least 7 days. The experimental protocol was approved by the Animal Ethical Committee of the University of Groningen (DEC 6427A).

Excision and preparation of mouse kidney slices

The protocol of the preparation and culture of kidney slices is illustrated in Figure 7 and a detailed description is given below.

Preparation of Krebs–Henseleit buffer (KHB)

KHB was used as slicing buffer, and 10 l of a 10× concentrated KHB stock solution (10× KHB) were prepared by first dissolving 36.7 g $CaCl_2 \cdot 2H_2O$ in 5 l of ultrapure water (solution 1). Then, 37.3 g KCl, 690 g NaCl, 27.1 g $MgSO_4 \cdot 7H_2O$ and 16.3 g KH_2PO_4 were dissolved in ultrapure water to a volume of 5 l (solution 2). Subsequently, solutions 1 and 2 were mixed and filtered through a 0.45-µm filter. This 10× KHB can be stored at 4°C for about 6 months. On the day of slicing, 5 l 1× KHB were prepared by dissolving 10.5 g $NaHCO_3$ (Merck, Darmstadt, Germany), 24.75 g D-glucose monohydrate (Merck, Darmstadt, Germany) and 11.9g HEPES (MP Biomedicals, Aurora, OH, USA) in ~2 l of ultrapure water at 4°C. Then, 500 ml 10× KHB and ultrapure water at 4°C were added to yield a final volume of 5 l. This solution was kept at 0-4°C on melting ice, and was oxygenated with 95% O_2/5% CO_2 for 30 min on ice, using a gas dispersion tube with a fritted disc. The pH of the solution was adjusted to 7.42 by slowly adding 5 N NaOH solution. This solution can be stored for 24 h at 4°C. Before use, the buffer was reoxygenated and the pH was readjusted.

Williams medium E glutamax-I (WME) slice incubation medium

On the day of the experiment, slice incubation medium was prepared by adding 1.375 g D-glucose monohydrate (Merck, Darmstadt, Germany) and 500 µl gentamicin (50 mg/ml) (Invitrogen, Paisley, UK) to 500 ml Williams medium E with GlutaMAX (Invitrogen, Paisley, UK). If necessary, this solution can be stored for 24 h at 4°C.

Slicing procedure

Preparations before start of slicing

KHB for slicing and WME (plus supplements) incubation medium were prepared as described above. WME incubation medium was transferred into culture plates, with 12-well plates requiring 1.3 ml of culture medium per well to support the tissue for 24 h. The volume-to-surface ratio of the culture medium is of great importance for optimal exchange of O_2 and CO_2 between the culture medium and the atmosphere of 80% O_2/5% CO_2, and the ratio of tissue to volume is important for sufficient supply of nutrients. The plates were pre-warmed and oxygenated by placing them in the shaking incubator at 37°C under 80% O_2/5% CO_2 for at least 30 min. The Krumdieck slicer (Alabama Research and Development, USA) was assembled according to the manufacturer's instructions and pre-cooled by recirculating cooled water (4°C) through the cooling block, using a refrigerated circulator bath.

Collection of kidney tissue

Mice were anesthetized under 2% isofluorane/O_2 (Nicholas Piramal, London, UK), the right and left kidneys were retrieved as quickly as possible and placed into ice-cold University of Wisconsin (UW) organ preservation solution (DuPont Critical Care, Waukegab, IL, USA). All further steps up to incubation were performed on ice (at 0-4°C). The mouse kidneys were transferred to a Petri dish with a silicone insert in order to remove adipose tissue around the kidney. The whole kidney was then placed into the core cylinder.

Preparation of kidney slices

The slicer was filled with ice-cold oxygenated KHB through the glass-trap assembly. It was ensured that the buffer reached the level required for proper functioning of the pump and that the tissue core was completely submerged. For mouse kidney slices, whole kidneys were transferred from the ice-cold UW solution used for storage into the cylindrical core holder of the slicer.

Slices were cut using the Krumdieck slicer at a speed setting of 30-40. The wet weight of the first few slices was checked as an indication of slice thickness after carefully blotting the slices on a smooth, not too absorptive paper to remove adherent water, with an optimal wet weight of 5 mg.

If necessary, the cutting thickness was adjusted by turning the graduated thickness control knob until the required wet weight was reached. The slice thickness can be slightly increased by placing weights on top of the tissue core holder, which may also facilitate the slicing of hard (fibrotic) kidney tissue. Kidney slices that are too thick (>400 μm) may develop necrosis in the center of the slice, as the diffusion distance for nutrients and oxygen is too long. After slicing one core, the slices were removed from the glass trap by opening the tap, collecting them in a beaker and placing them immediately on ice. Slices were selected on the basis of their appearance, with good slices having an equal thickness, uniform color and smooth edges. Selected slices were transferred into fresh ice-cold UW and stored on ice.

A spatula (not forceps) was used to avoid damaging the slices. The KHB slicing buffer was replaced by fresh, ice-cold and oxygenated KHB every 15-30 min, and the knife was replaced when slice quality (judged by eye) decreased.

Experimental setup slice cultures

In this study three independent experiments were performed, each using four kidneys (2 mice) from which in total four cores were drilled. After slicing, slices were pooled before plating them for culture. ATP measurements were performed on single slices. For mRNA expression analysis, in each experiment slices were cultured in triplicate for each condition after which they were pooled for RNA isolation. Histological analyses were performed on single slices per condition in each experiment.

Incubation of kidney slices

Kidney slices were washed quickly by gently transferring them into WME to remove the UW. Before adding medium and mPCKS, 12 well plates were coated with 10% bovine serum albumin (BSA) in milliQ water for 30 minutes. The solution was removed and plates were air dried. Slices were then incubated in the coated plates containing per well 1.3 ml Williams Medium E glutamax-I (Gibco, Paisley, UK) per well supplemented with 25 mM D-glucose and 50 µg/ml gentamycin. Medium was pre-warmed and gassed with 80% O_2/5% CO_2 before it was added to the wells. Slices were individually transferred to the wells of a culture plate placed on a surgical mattress to maintain the medium at 37°C. Plates were immediately transferred back in a shaking CO_2 incubator (90 cycles/min) under continuous supply of 80% O_2/5% CO_2, as the pH of the medium rapidly changes in normal atmosphere. Slices were incubated for 1, 6, 12, 24, 48 or 72 h. When appropriate, after 24 and 48 h slices were transferred to new plates with fresh medium. For refreshing, new culture plates were filled with medium, and the plates were pre-warmed and oxygenated. The incubated plates and new plates were placed on a surgical mattress to maintain the temperature at 37°C. The slices were quickly transferred from the incubated plates into the new plates with a spatula and placed in the incubator.

Uptake of FITC-lysozyme by mPCKS

FITC-lysozyme was prepared as described before (Kok et al., 1998). Briefly, 500 µl of 1 mg/ml FITC (Thermo Scientific, Wilmington, USA) was carefully mixed with 5 ml of 2 mg/ml lysozyme solution (Sigma-Aldrich, Saint Louis, USA) for 8 h at 4 °C in the dark, dialysed against water and finally lyophilized. Mouse kidney slices were incubated up to 3 h with 1 mg/ml FITC-lysozyme. After 1 and 3 h, the mPCKS were embedded in Tissue-tek (Sakura, Japan) and snap-frozen in isopentane (-80 °C). They were stored at -80 °C until 4 µm cryosections were cut perpendicular to the surface of the slices. Cross-sections were allowed to dry on a glass microscope slide and covered with Citifluor (Citifluor Ltd., London, UK). Slides were examined using a high-end fully motorized Zeiss AxioObserver Z1 microscope and images were acquired using TissueFAXS Image Analysis Software (TissueGnostics, Austria). Images were converted to red/green pseudo-colours using lookup tables in ImageJ 1.47v (http://imagej.nih.gov/ij).

Induction of renal pre-fibrosis ex vivo

In order to induce renal pre-fibrosis *ex vivo,* slices were incubated for 48 h in the presence of recombinant human TGFβ1 (5 ng/ml, hTGFβ1, Roche, Mannheim, Germany). Medium without TGFβ1 was used for comparison. After 24 h of incubation, slices were transferred to new coated plates with fresh medium containing TGFβ1.

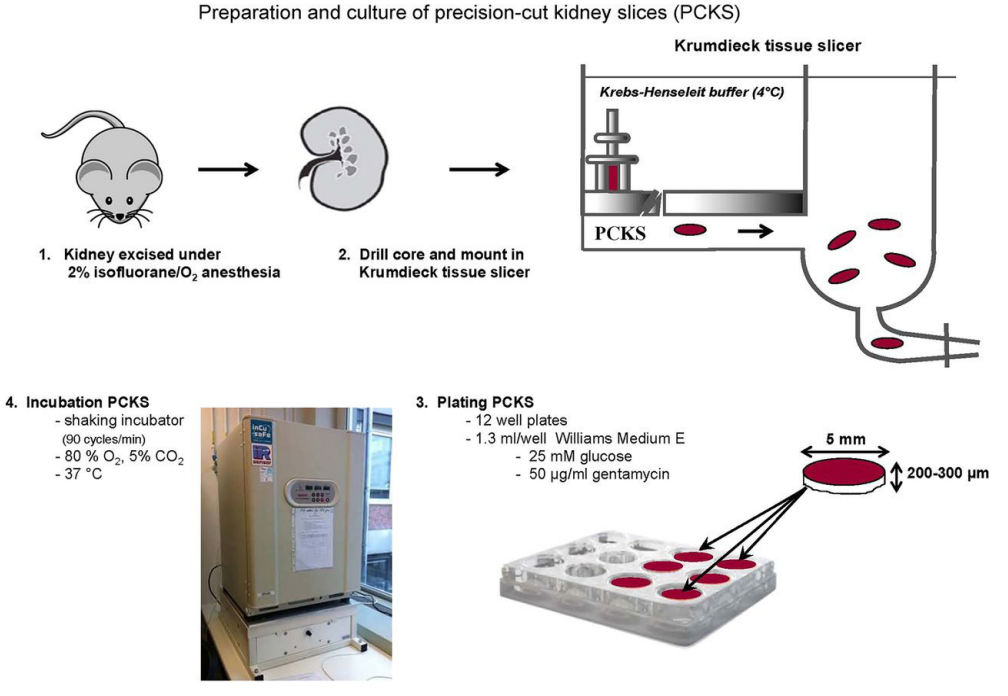

Figure 7. Schematic representation of the experimental approach for obtaining and culturing mPCKS. (1) Mouse kidneys (n = 3) were excised under isofluorane/O_2 anesthesia and placed into ice-cold UW preservation solution. (2) Cores were drilled and immediately transferred to the cylindrical core holder of a Krumdieck slicer and cut into 5-mm diameter slices. (3) High-quality slices (equal thickness at all sides and smooth edges) were transferred to 12-well plates using a spatula to avoid damaging of the slices, and (4) were placed in a shaking (90 cycles/min) incubator under continuous supply of 80% O_2/5% CO_2 at 37°C.

Synthesis of conjugates

PPB-PEG-IFNγ (in which PPB is the PDGFR recognizing binding peptide) was synthesized as described previously (Bansal et al., 2011a). Briefly, for PPB-

PEG-IFNγ, recombinant murine IFNγ (0.256 nmol, Peprotech, London, UK) was mixed with 12.8 nmol of maleimide-PEG-succinimidyl carboxy methyl ester (Mal-PEG-SCM, 2 KDa, Creative PEGworks, Winston-Salem, NC) for 2 h and dialyzed overnight against PBS using 10 KDa dispodialyzer (Harvard Apparatus, Holliston, Massachusetts, USA). The dialyzed sample was then mixed with SATA (succinimidyl acetyltioacetate)-modified PPB (PPB-ATA, 25.6 nmol) in the presence of a deacetylating reagent. Finally, PPB-PEG-IFNγ was extensively dialyzed against PBS and stored at -80°C.

For PPB-HSA, human serum albumin (HSA, 1.5 µmol dissolved in PBS) was mixed with γ-maleimidobutyryloxy-succinimide ester (GMBS, 30 µmol, dissolved in DMF) for 2 h and extensively dialyzed against PBS using 10 KDa cut-off dialysis membrane cassette (Thermo Scientific, Rockford, IL, USA). Next, PPB-ATA (34.5 µmol; dissolved in DMF) was added to the GMBS-modified HSA for overnight, and dialyzed against PBS. The final product (PPB-HSA) was freeze-dried for storage at -20°C.

Antifibrotic effects of free IFNγ and PPB-PEG-IFNγ

To determine the antifibrotic effects of free IFNγ and PPB-PEG-IFNγ, slices were incubated for 48 h with free IFNγ, PPB-PEG-IFNγ, PPB-HSA (equivalent 1 µg/ml) or medium alone in the presence or absence of TGFβ1 as described above. After the first 24 h of incubation slices were transferred to new 12 well plates with fresh medium containing TGFβ1 and the respective antifibrotic compounds. TGFβ1 and IFNγ constructs were administered simultaneously. The concentration of 1 µg/ml of IFNγ constructs was chosen based on results from previous *in vitro* experiments (Bansal et al., 2011a; Poosti et al., 2014).

Viability of mPKCS: ATP and protein content

The general viability of the PCKS during culture was determined by measuring ATP content of the slices. For ATP measurements, single slices were transferred to a sonication solution containing 70% ethanol (v/v) and 2 mM EDTA (pH 10.9), snap-frozen in liquid nitrogen and stored at -80°C until analysis. After homogenization using a Mini-BeadBeater-8 (BioSpec, Bartlesville, OK, USA), the samples were centrifuged for 2 min. at 13000 rpm. The supernatant was diluted 10 times with

0.1 M Tris–HCl/2 mM EDTA buffer (pH 7.8) to lower the ethanol concentration and used to measure ATP contents using the ATP Bioluminescence assay kit CLSII (Roche diagnostics, Mannheim, Germany) according to the manufacturer's protocol. The remaining pellet was used to determine the protein content of the mPCKS by dissolving it in 200 µL of 5 M NaOH for 30 minutes. After dilution with water to a concentration of 1 M NaOH, the protein content of the samples was determined using the Lowry method (Bio-Rad DC Protein Assay, Bio-Rad, Munich, Germany). BSA was used for the calibration curve. ATP values (in pmol) were divided by the total protein content (in µg) of the respective slices and expressed as the ratio ATP/protein.

Quantitative Real-Time PCR

In order to determine TGFβ-induced pre-fibrosis, and to examine the effect of IFNγ and PPB-PEG-IFNγ, gene expression of fibrosis markers [*alpha smooth muscle actin (α-SMA)*, *fibronectin (Fn)*, *collagens I & III*] was measured using quantitative Real-Time (qRT) PCR. The triplicate slices were pooled and snap-frozen. Total RNA from kidney slices was extracted using the RNeasy Mini Kit (Qiagen, Hilden, Germany) according to the manufacturer's instructions. The RNA concentrations were measured on a NanoDrop ND-1000 spectrophotometer (Thermo Scientific, Wilmington, USA). Single-stranded cDNA was synthesized using Superscript II and random hexamer primers (Invitrogen, Carlsbad, CA, USA) in a volume of 20 µl. cDNA was first diluted to a concentration of 2 ng/µl and 2.5 µl/reaction (5 ng) and was then used for qRT-PCR analysis. PCR reactions were performed in a 10 µl reaction volume containing 1 x qPCR master mix (Eurogentec, Liege, Belgium) and 1x TaqMan Gene Expression Assay mix (Applied Biosystems, Forster City, CA, USA). The TaqMan assay numbers were as follows: *Ywhaz*: Mm03950126_s1, *Col1a1*: Mm00801666_g1, *Col3a1*: Mm01254476_m1, α-*SMA/Acta2*: Mm01546133_m1, *Fn*: Mm01256744_m1, MHCII/CD74: Mm00658576_m1. qRT-PCR reactions were performed on a ABI7900HT thermal cycler (Biosystems, Forster City, CA, USA). Relative gene expression was calculated using the $2^{-\Delta Ct}$ method with *Ywhaz* (tyrosine 3-monooxygenase/tryptophan 5-monooxygenase activation protein) as housekeeping gene.

Histology of mPKCS

Study of histological changes was performed on 2 µm sections from formalin-fixed paraffin-embedded slices. For immunohistochemistry the following primary antibodies were used: anti-alpha smooth muscle actin (α-SMA, clone ASM-1, Progen Biotechnik, Heidelberg, Germany); anti-fibronectin (ab6584, Abcam, Cambridge, UK); and anti-collagen III (s1330-01, SouthernBiotech, Birmingham, Alabama, USA). Sections were deparaffinised in xylene and rehydrated in graded alcohol and distilled water. Antigen retrieval was achieved by overnight incubation at 60ºC in 0.1 M Tris/HCl buffer (pH 9.0) for fibronectin and collagen III staining. No antigen retrieval was performed for α-SMA staining. Endogenous peroxidase activity was blocked with 0.03% H_2O_2 (in PBS) for 30 min. Primary antibody binding was detected by sequential incubations with horseradish peroxidase (HRP)-labeled appropriate secondary and tertiary antibodies (obtained from DAKO, Glostrup, Denmark). Peroxidase activity was visualized using 3,3'-diaminobenzidine tetrahydrochloride (DAKO, Glostrup, Denmark) as chromogen (10 min incubation). Sections were counterstained with haematoxylin for 1 minute and mounted with Kaiser's glycerin gelatin.

Quantification of immunostaining

To quantify immunostaining of fibronectin and collagen III, sections were first scanned using a NanoZoomer HT (Hamamatsu Photonics K.K., Shizuoka Pref., Japan). Next, the extent of fibronectin and collagen III positive staining was measured (number of positive pixels) using Aperio ImageScope software (version 9.1.772.1570, Aperio Technologies Inc, Vista, CA, USA).

Statistical analyses

Statistical analyses were performed using GraphPad Prism 5.0 (GraphPad Software Inc, La Jolla, CA, USA). Data are expressed as mean ± standard error of the mean of three independent experiments. Differences between multiple groups were calculated using ANOVA. Comparisons of two groups were performed using Student's t-test. $p < 0.05$ was considered statistically significant.

REFERENCES

1. **Bansal, R., Prakash, J., Post, E., Beljaars, L., Schuppan, D., and Poelstra, K.** (2011) Novel engineered targeted interferon-gamma blocks hepatic fibrogenesis in mice. *Hepatology* **54**, 586-596.
2. **Bansal, R., Post, E., Proost, J. H., de Jager-Krikken, A., Poelstra, K., and Prakash, J.** (2011) PEGylation improves pharmacokinetic profile, liver uptake and efficacy of interferon gamma in liver fibrosis. *J. Control. Release* **154**, 233-240.
3. **Bansal, R., Prakash, J., de Ruijter, M., Beljaars, L., and Poelstra, K**. (2011) Peptide-modified albumin carrier explored as a novel strategy for a cell-specific delivery of interferon gamma to treat liver fibrosis. *Mol Pharm*. **8**, 1899-1909
4. **Bansal, R., Tomar, T, Ostman, A., Poelstra, K., and Prakash, J.** (2012) Selective targeting of interferon gamma to stromal fibroblasts and pericytes as a novel therapeutic approach to inhibit angiogenesis and tumor growth. *Mol. Cancer Ther*. **11**, 2419-2428.
5. **Basile, D. P., Leonard, E. C., Beal, A. G., Schleuter, D., and Friedrich, J.** (2012) Persistent oxidative stress following renal ischemia-reperfusion injury increases ANG II hemodynamic and fibrotic activity. *Am. J. Physiol. Renal. Physiol*. **302**, F1494-502.
6. **Boor, P., Ostendorf, T., and Floege, J.** (2010) Renal fibrosis: Novel insights into mechanisms and therapeutic targets. *Nat. Rev. Nephrol.* **6**, 643-656
7. **Cleland, J. L., and Jones, A. J.** (1996) Stable formulations of recombinant human growth hormone and interferon-gamma for microencapsulation in biodegradable microspheres. *Pharm. Res*. **13**, 1464-1475.
8. **de Graaf, I. A., Olinga, P., de Jager, M. H., Merema, M. T., de Kanter, R., van de Kerkhof, E. G., and Groothuis, G. M.** (2010) Preparation and incubation of precision-cut liver and intestinal slices for application in drug metabolism and toxicity studies. *Nat. Protoc*. **5**, 1540-51
9. **de Kanter, R., Monshouwer, M., Meijer, D. K., and Groothuis, G. M.** (2002) Precision-cut organ slices as a tool to study toxicity and metabolism of xenobiotics with special reference to non-hepatic tissues. *Curr. Drug Metab*. **3**, 39-59.
10. **de Kanter, R., Tuin, A., van de Kerkhof, E., Martignoni, M., Draaisma, A. L., de Jager, M. H., de Graaf, I. A., Meijer, D. K., and Groothuis, G.M.** (2005) A new technique for preparing precision-cut slices from small intestine and colon for drug biotransformation studies. *J. Pharmacol. Toxicol. Methods.* **51**, 65-72.
11. **Duffield, J. S.** (2014) Cellular and molecular mechanisms in kidney fibrosis. *J. Clin. Invest.* **124**, 2299-2306
12. **Eddy, A.A.** Suppl (2011). 2014 Overview of the cellular and molecular basis of kidney fibrosis. *Kidney Int*. **4**, 2-8.
13. **Farrar, M. A., and Schreiber, R. D.** (1993) The molecular cell biology of interferon-gamma and its receptor. *Annu. Rev. Immunol*. **11**, 571-611.
14. **Flamant, M., Placier, S., Rodenas, A., Curat, C. A., Vogel, W. F., Chatziantoniou, C., and Dussaule, J. C.** (2006) Discoidin domain receptor 1 null mice are protected against hypertension-induced renal disease. *J.*

Am. Soc. Nephrol. **17**, 3374-3381.

15. **Friedman, S. L., Sheppard, D., Duffield, J. S., and Violette, S.** (2013) Therapy for fibrotic diseases: Nearing the starting line. *Sci. Transl. Med*. **5**, 167sr1.

16. **Gu, F., Younes, H. M., El-Kadi, A. O., Neufeld, R. J., and Amsden, B. G.** (2005) Sustained interferon-gamma delivery from a photocrosslinked biodegradable elastomer. *J. Control. Release* **102**, 607-617.

17. **Hadi, M., Westra, I. M., Starokozhko, V., Dragovic, S., Merema, M. T., and Groothuis, G. M.** (2013) Human Precision-Cut Liver Slices as an *ex Vivo* Model to Study Idiosyncratic Drug-Induced Liver Injury. *Chem. Res. Toxicol*. **26**, 710-720.

18. **King, T. E.,Jr, Albera, C., Bradford, W. Z., Costabel, U., Hormel, P., Lancaster, L., Noble, P. W., Sahn, S. A., Szwarcberg, J., Thomeer, M., et al.** (2009) Effect of interferon gamma-1b on survival in patients with idiopathic pulmonary fibrosis (INSPIRE): A multicentre, randomised, placebo-controlled trial. *Lancet*. **374**, 222-228.

19. **LeBleu, V. S., Taduri, G., O'Connell, J., Teng, Y., Cooke, V. G., Woda, C., Sugimoto, H., and Kalluri, R.** (2013) Origin and function of myofibroblasts in kidney fibrosis. *Nat. Med*. **19**, 1047-1053.

20. **Lee, J., Lee, J., Park, M. K., Lim, M. A., Park, E. M., Kim, E. K., Yang, E. J., Lee, S. Y., Jhun, J. Y., Park, S. H., et al.** (2013) Interferon gamma suppresses collagen-induced arthritis by regulation of Th17 through the induction of indoleamine-2,3-deoxygenase. *PloS One*. **8**, e60900.

21. **Levey, A. S., Atkins, R., Coresh, J., Cohen, E. P., Collins, A. J., Eckardt, K. U., Nahas, M. E., Jaber, B. L., Jadoul, M., Levin, A., et al.** (2007) Chronic kidney disease as a global public health problem: Approaches and initiatives - a position statement from kidney disease improving global outcomes. *Kidney Int*. **72**, 247-259.

22. **Nagae, T., Mori, K., Mukoyama, M., Kasahara, M., Yokoi, H., Suganami, T., Sawai, K., Yoshioka, T., Koshikawa, M., Saito, Y., et al.** (2008) Adrenomedullin inhibits connective tissue growth factor expression, extracellular signal-regulated kinase activation and renal fibrosis. *Kidney Int*. **74**, 70-80.

23. **Oldroyd, S. D., Thomas, G. L., Gabbiani, G., and El Nahas, A. M.** (1999) Interferon-gamma inhibits experimental renal fibrosis. *Kidney Int*. **56**, 2116-2127.

24. **Poosti, F., Bansal, R., Yazdani, S., Prakash, J., Post, E., Klok, P., van den Born, J., de Borst, H. M., van Goor, H., Poelstra, K. et al.** (2015). Selective delivery of interferon gamma to renal interstitial myofibroblasts: a novel strategy for the treatment of renal fibrosis. FASEB J. **29**, 1029-1042.

25. **Strutz, F., Heeg, M., Kochsiek, T., Siemers, G., Zeisberg, M., and Muller, G. A.** (2000) Effects of pentoxifylline, pentifylline and gamma-interferon on proliferation, differentiation, and matrix synthesis of human renal fibroblasts. *Nephrol. Dial. Transplant*. **15**, 1535-1546.

26. **Strutz, F., and Zeisberg, M.** (2006) Renal fibroblasts and myofibroblasts in chronic kidney disease. *J. Am. Soc. Nephrol*. **17**, 2992-2998.

27. **Tharaux, P. L., Chatziantoniou, C., Fakhouri, F., and Dussaule, J. C.** (2000) Angiotensin II activates collagen I gene through a mechanism involving the MAP/ER kinase pathway. *Hypertension* **36**, 330-336.

28. **van de Kerkhof, E. G., de Graaf, I. A., de Jager, M. H., Meijer, D. K., and Groothuis, G. M.** (2005) Characterization of rat small intestinal and colon precision-cut slices as an *in vitro* system for drug metabolism and induction studies. *Drug Metab. Dispos*. **33**, 1613-1620.

29. **van Swelm, R.P., Hadi, M., Laarakkers, C.M., Masereeuw, R., Groothuis, G.M., and Russel, F. G.** (2014) Proteomic profiling in incubation medium of mouse, rat and human precision-cut liver slices for biomarker detection regarding acute drug-induced liver injury. *J. Appl. Toxicol*. **34**, 993-1001.

30. **Vickers, A. E., Fisher, R. L.** (2005) Precision-cut organ slices to investigate target organ injury. *Expert Opin. Drug Metab. Toxicol*. **1**, 687-699.

31. **Weng, H. L., Wang, B. E., Jia, J. D., Wu, W. F., Xian, J. Z., Mertens, P. R., Cai, W. M., and Dooley, S.** (2005) Effect of interferon-gamma on hepatic fibrosis in chronic hepatitis B virus infection: A randomized controlled study. *Clin. Gastroenterol. Hepatol*. **3**, 819-828.

32. **Westra, I. M., Pham, B. T., Groothuis, G. M., and Olinga, P.** (2013) Evaluation of fibrosis in precision-cut tissue slices. *Xenobiotica* **43**, 98-112.

33. **Westra, I. M., Oosterhuis, D., Groothuis, G. M., and Olinga, P.** (2014) The effect of antifibrotic drugs in rat precision-cut fibrotic liver slices. *PLoS One* **9**, e95462.

34. **Westra, I. M., Oosterhuis, D., Groothuis, G. M., and Olinga, P**. (2014) Precision-cut liver slices as a model for the early onset of liver fibrosis to test antifibrotic drugs. *Toxicol. Appl. Pharmacol*. **274**, 328-338.

35. **Yao, Y., Zhang, J., Tan, D. Q., Chen, X. Y., Ye, D. F., Peng, J. P., Li, J. T., Zheng, Y. Q., Fang, L., Li, Y. K., et al.** (2011) Interferon-gamma improves renal interstitial fibrosis and decreases intrarenal vascular resistance of hydronephrosis in an animal model. *Urology*. **77**, 761.e8-761.e13.